

Formation of CO in the Reaction of O Atom With CH₃: Reaction Over a Barrier but Not Through a Saddle Point

Vadim D. Knyazev

Department of Chemistry, The Catholic University of America, Washington, D. C. 20064, and
National Institute of Standards and Technology, Physical and Chemical Properties Division,
Gaithersburg, MD 20899

Traditionally, the exploration of mechanisms of reactions and, consequently, the computation of related rate parameters have concentrated on identifying and studying properties of saddle points on potential energy surfaces (PES) of reactive systems. This predominant attention to PES saddle points is based on two paradigmatic postulations. First is the identification of the minimum energy path connecting the reactants and the products of a particular reaction channel with the reaction coordinate. The reaction coordinate itself can be defined mathematically in different ways but it is generally associated with the length along the intuitive “reaction path” describing the transformation of the reactive system in its motion from reactants to products. The second assumption is that this minimum energy path, at least in the vicinity of the energy barrier, represents a local minimum of PES in all directions (degrees of freedom) except for the one that corresponds to the “reaction coordinate,” thus forming a valley on the PES. If an energy barrier is present, then this valley path, crossing over the barrier, necessarily passes through a PES saddle point. This second assumption is usually taken as self-evident and thus avoids discussion. One exception is the issue of reaction path bifurcations, such as those occurring at valley-ridge inflection points, which has received significant attention. The local minimum/valley/saddle point assumption is correct for the lowest energy channel but is not necessarily valid for the higher energy channels. For the lowest energy channel, any trajectory adjacent (in coordinate space) to that passing through a saddle point proceeds to the same products but over a slightly higher energy barrier. One can, however, imagine a system where two adjacent trajectories that pass over the energy barrier (separating the reactant and the product valleys) in the vicinity of a bifurcation point proceed to different product sets. This situation is illustrated in Figure 1. Figure 1a depicts a “traditional” reactive system with two channels, each characterized by its corresponding saddle point (TS1 and TS2). Figure 1b presents a reactive system where only the lowest energy channel has an associated saddle point. The bifurcation point on the potential energy surface “ridge” is shown by the vertical line. Trajectories that pass over the ridge to the left of this line proceed to the products of the second channel while those that cross the PES ridge on the right side of this bifurcation point are a part of the reaction flux representing the first, lowest-energy, reaction channel.

This article presents RRKM-theory¹⁻³ based calculations of the microscopic energy-dependent rate constants and branching fractions of a unimolecular reaction channel without a saddle point. The particular reactive system considered is that of the channel of formation of CO in the reaction of O atoms with CH₃ radicals.

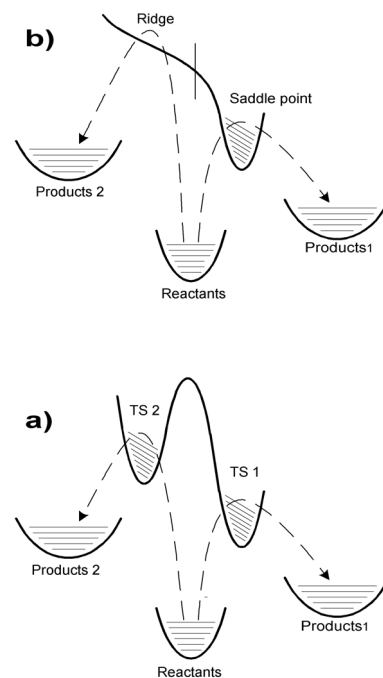
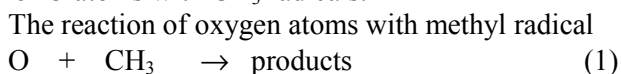


Figure 1. Qualitative character of the PES for reactions proceeding over an energy barrier but not through PES saddle points.

is an important part of the complex mechanism of combustion of hydrocarbon fuels.^{4,5} Several experimental studies (refs ⁶⁻¹³, also see reviews in refs ¹⁴ and ¹⁵) resulted in an overall rate constant $1.4 \times 10^{-10} \text{ cm}^3 \text{ molecule}^{-1} \text{ s}^{-1}$, independent of temperature. The widest temperature range was covered in the experiments of Slagle et al.⁹ who isolated reaction 1 for direct study by the Laser Photolysis / Photoionization Mass Spectrometry (LP/PIMS) technique between 294 and 900 K at low pressures.

It has been generally assumed that the only channel of reaction 1 is that producing formaldehyde (detected in several of the above experimental studies) and hydrogen atom:



In 1992 Seakins and Leone¹⁶ detected the formation of vibrationally excited CO (CO vibrational temperature of $12700 \pm 1400 \text{ K}$) in their room temperature Laser Photolysis / FTIR emission study of reaction 1, thus providing experimental evidence for the existence of a second channel



Recent Laser Photolysis / Laser Induced Fluorescence experiments of Min et al.¹⁷ have confirmed the formation of excited CO in reaction 1, providing, however, a significantly lower degree of CO vibrational excitation, that corresponding to a vibrational temperature of about 2000 K.

The values of the reaction channel 1b branching ratio were reported by several groups. Seakins and Leone obtained $40 \pm 10\%$ branching fraction for CO formation by comparing the IR emission signal intensities of several of the lowest vibrational levels of CO obtained in reaction 1b with those of CO originating from the acetone photolysis. In 1999, Fockenberg et al.¹³ studied reaction 1 at room temperature and 133 Pa (1 torr) using the LP/PIMS technique with a time-of-flight mass spectrometer. These authors reported $17 \pm 11\%$ branching fraction for reaction channel 1b. In a subsequent work by the same group,¹⁸ this value was refined ($18 \pm 4\%$) by using diode laser absorption experiments with isotopically substituted acetone as a source of CH_3 radicals and reference concentrations of ^{13}CO . Slagle et al.¹⁹ used the LP/PIMS method to determine the branching fraction of reaction channel 1a by monitoring the formation of formaldehyde, the major product of reaction 1. The reported value of channel 1a branching fraction, $85 \pm 15\%$, results in the 0 – 30% range of possible values of the fraction of the CO-producing channel 1b.

In spite of the experimentally proven importance of the CO-producing reaction channel 1b, theoretical attempts to locate a corresponding transition state have failed.¹⁹ The initial act of reaction 1 is believed to be the addition of O atom to the CH_3 radical with the formation of a highly vibrationally excited CH_3O radical ($\Delta H_{298}^0 = -378 \text{ kJ mol}^{-1}$). This excited radical subsequently undergoes rapid decomposition to products via a chemically activated mechanism. Collisional stabilization is not expected to be important under any experimentally achievable conditions due to the very large decomposition rates. The reaction pathway corresponding to channel 1a is that of simple H elimination from CH_3O (the reaction energy barrier is likely to be in the $107 - 143 \text{ kJ mol}^{-1}$ range, see review in ref ¹⁶). The most plausible pathway resulting in the formation of CO is the initial elimination of H_2



Since reaction channel 1c leaves 354 kJ mol^{-1} to be distributed among the two products and the C-H bond of HCO is only 70 kJ mol^{-1} ,^{20,21} channel 1c, most likely, will be followed by the immediate decomposition of excited HCO producing H and CO



In the theoretical part of the study of Slagle et al.,¹⁹ attempts were made to locate a transition state (PES saddle point) that would lead to the products of reaction channels 1b or 1c. None, however, could be found. As will be demonstrated in the current work, there exists no PES saddle point connecting the $\text{O} + \text{CH}_3$ reactants with the $\text{H}_2 + \text{HCO}$ products. Instead, reaction channel 1c (which will lead, via reaction 2, to the final products of channel 1b, $\text{H}_2 + \text{H} + \text{CO}$) proceeds through the area on the PES that involves crossing over an energy barrier (PES “ridge”) but has no associated saddle point. Since the study of reaction 1 in this article is mostly concerned with the transformations of the excited CH_3O adduct, the following reaction channel numbering will also be used:





Potential energy surface of the O + CH₃ system

The study of the potential energy surface (PES) of the O + CH₃ system was performed with an emphasis placed on the routes of decomposition of the CH₃O adduct formed in the initial reaction act. A relaxed scan of the PES was performed using four methods: UHF, UMP2, QCISD, and density functional B3LYP method with the 6-311G(d,p) basis set. The system of coordinates was designed to facilitate the description of the H₂-eliminating channel. Two variables, HX (half the H–H distance of the departing H₂ molecule) and XC (the distance between the C atom and the middle of the forming H-H bond), were fixed at a series of equidistant periodic values while the rest of the variables were optimized. The Gaussian 98 system of programs²² was used in all quantum chemistry calculations.

Qualitative shapes of PES

The results of PES scans performed using the above four methods, in spite of the different values of energy barriers, yielded similar results in terms of the qualitative description of the major PES properties. Figure 2 presents a 3-dimensional surface and contour plots (energy as a function of HX and XC) of the PES obtained at the UMP2/6-311G(d,p) level. Valleys A, B, and C represent the CH₃O adduct, H+H₂CO, and H₂+HCO, respectively. The saddle point TS1 is the transition state for the decomposition of CH₃O to H + H₂CO (reaction 3a); TS2 is the transition state for the abstraction reaction H + H₂CO → H₂ + HCO. There is no saddle point corresponding to the transition state of reaction 3b, i.e., the transformation leading from the CH₃O adduct to the H₂ + HCO products. However, as can be seen from Figure 2, the PES ridges between the A (CH₃O) and B (H+H₂CO) valleys and between the B (H+H₂CO) and C (H₂+HCO) valleys converge at low values of HX and XC and form a single ridge that separates the valleys A (CH₃O) and C (H₂+HCO). The wide cross-hatched line marked as TS3 represents the approximate location of this PES ridge. Trajectories originating in the reactant valley (A) and crossing this ridge are likely to proceed to the H₂+HCO products, thus representing reaction channel 3b.

Dividing surface

The hypothesis that the TS3 region of the PES represents the dividing surface between the A and the B valleys was verified by performing IRC²³ calculations in mass-weighted internal coordinates²⁴ using locations in the vicinity of TS3 as starting points. A line was drawn in the HX-XC coordinate plane in such a way that IRCs originating at small distances on one side of the line converged to the CH₃O valley and those originating on the other side proceeded either to H+H₂CO or to H₂+HCO. This analysis was performed using the PES obtained at the UMP2/6-311G(d,p) and

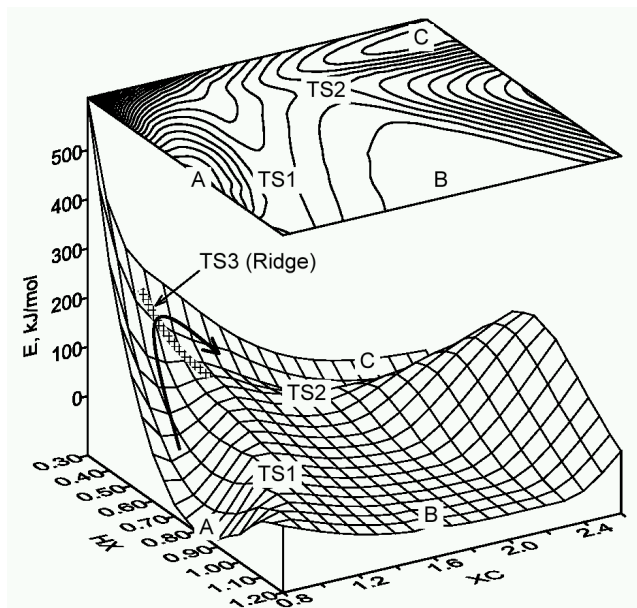


Figure 2. 3-dimensional surface and contour plots (energy as a function of HX and XC) of the PES obtained at the UMP2/6-311G(d,p) level. Valleys A, B, and C represent the CH₃O adduct, H+H₂CO, and H₂+HCO, respectively. Saddle points TS1 and TS2 are the transition states for the decomposition of CH₃O to H + H₂CO and for the abstraction reaction H + H₂CO → H₂ + HCO, respectively. There is no saddle point corresponding to the transition state of the CH₃O → H₂ + HCO (3b) reaction. However, the PES ridges between the A and B valleys and between the B and C valleys converge at low values of HX and XC and form a single ridge that separates the valleys A (CH₃O) and C (H₂+HCO). The wide cross-hatched line marked as TS3 represents the approximate location of this PES ridge. Trajectories originating in the reactant valley (A) and crossing this ridge are likely to proceed to the H₂+HCO products (as indicated by the curved arrow), thus representing reaction 3b.

density functional B3LYP/6-311G(d,p) levels. The resultant dividing line was taken as representing the PES ridge separating the reactant and the product valleys. The part of the dividing line with $HX < 0.425$ (UMP2 surface) or $HX < 0.455$ (B3LYP surface) was identified with the dividing surface for reaction 3b ($\text{CH}_3\text{O} \rightarrow \text{H}_2 + \text{HCO}$); the remaining part of the line with $HX > 0.425$ (UMP2 surface) or $HX > 0.455$ (B3LYP surface) was taken as representing the dividing surface for the decomposition of CH_3O to $\text{H} + \text{H}_2\text{CO}$, reaction 3a.

To obtain a more accurate evaluation of the potential energy profile along the PES ridge, single-point G2²⁵ and CBS-Q²⁶ calculations were performed for several configurations along the “ridge line” and for the CH_3O equilibrium configuration. The resultant potential energy profiles along the dividing line are shown in Figure 3. As can be seen from the plots, the G2 and the CBS-Q level profiles differ very little (less than 4.3 and 2.5 kJ mol^{-1} with the UMP2- and the B3LYP-level surfaces, respectively).

Energy-dependent rate constants $k(E)$ and branching fractions for channels 1a and 1c.

Projected^{27,28} vibrational frequencies were calculated for the same sequence of points on the dividing line as was used in the $V(q)$ calculation above (Table 1). Calculations were performed using both the UMP2 and the B3LYP method. The energy-specific rate constants $k(E)$ for channels 3a and 3b were obtained by the method developed by Knyazev²⁹ for reactions occurring over PES ridges but not through saddle points. The method is based on integration (or summation) of the sum-of-states functions obtained along the separating PES ridge. $k(E)$ calculations were performed using four models: those resulting from the G2 and CBS-Q potential energy profiles along the dividing lines obtained on the UMP2 and B3LYP potential energy surfaces. The resultant $k_{3a}(E)$ and $k_{3b}(E)$ dependences obtained with the B3LYP potential energy surface are presented in Figure 4. Also shown in Figure 4 is the dependence on energy of the energy-specific branching ratio of channels 3b and 3a, $\gamma(E) = k_{3b}(E)/k_{3a}(E)$. $\gamma(E)$ increases with energy, reaching the values of 0.025 (0.027) and 0.048 (0.050) (obtained with the G2 (CBS-Q) energy profiles along the dividing line obtained on the UMP2 and B3LYP PES, respectively) at the energy of 372 kJ mol^{-1} , which corresponds to the energy of the “entrance” barrier of the chemically activated reaction



These values of $\gamma(E)$ result in a 2.5% – 5% branching fraction of the CO-producing channel 1b since the HCO molecule produced in reaction channel 1c is expected to instantly decompose due to the high

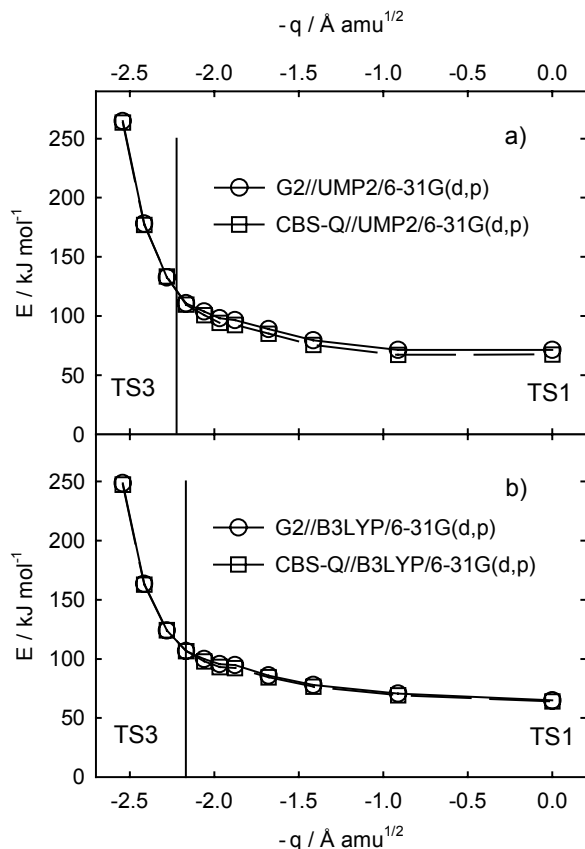


Figure 3. (a) Energy values calculated using the G2 (circles and solid line) and CBS-Q (squares and dashed line) methods at selected points along the dividing line (PES ridge) on the UMP2 surface. Energy values include the zero-point vibrational energy and are given relative to CH_3O . The part of the PES ridge to the left of the vertical line represents the dividing surface (TS3) for reaction 3b ($\text{CH}_3\text{O} \rightarrow \text{H}_2 + \text{HCO}$) and that to the right of the vertical line corresponds to the dividing surface (TS1) for reaction 3a ($\text{CH}_3\text{O} \rightarrow \text{H} + \text{H}_2\text{CO}$). (b) The same as in part (a) but for the B3LYP-level potential energy surface.

exothermicity of reaction 1c (354 kJ mol^{-1}) which exceeds the barrier for HCO decomposition (70 kJ mol^{-1}) by a factor of five.

Discussion.

This work, to the best of the author's knowledge, is the first attempt to apply a statistical rate theory to quantitatively model reactions that are characterized by energy barriers but have no associated saddle points on the PES. Traditionally, exploration of the mechanisms of chemical reactions via computational methods have concentrated on identification of the PES saddle points and the majority of the mathematical methods of PES analysis developed hitherto serve this purpose. The example of reaction 1c presented in this work demonstrates the importance of reactions without saddle points. One type of reactive system where such "over-the-ridge" reactions can be of significant importance is that of chemically activated reactions with large differences between the "entrance" and the "exit" barriers. In such systems, the energy barrier differences between different channels of decomposition of the adduct can be less important for the competition between these channels than the differences in the entropic (or preexponential) factor. Thus, higher-energy "over-the-ridge" channels may make noticeable contributions.

The applicability of statistical theories of chemical reactions, such as RRKM, to processes that are as fast as the decomposition of the excited CH_3O formed in the CH_3+O reaction ($k(E) \approx 10^{12} - 10^{14} \text{ s}^{-1}$) is doubtful. The decomposition of CH_3O^* occurs on a time scale that is too short to allow for full randomization of energy. In this respect, comparing rates of individual channels may still be meaningful in spite of the fact that the RRKM formula for $k(E)$ is not valid. Assessment of the relative importance of channels requires only a relaxed ergodicity assumption: that, in the transition states, all states of equal energy are reached with equal probability by the trajectories originating from the excited CH_3O molecule. No assumption of a random energy redistribution within the molecule's phase space is required.

The values of the fraction of channel 1b (originating from the decomposition of HCO produced in channel 1c) calculated in the current work (2.5% and 5%, depending on the potential energy surface used) are significantly lower than the experimental values of Seakins and Leone,¹⁶ Fockenberg et al.,¹³ and Preses et al.¹⁸ ($40 \pm 10\%$, $17 \pm 11\%$, and $18 \pm 4\%$, respectively). The level of agreement with experiment can be only be characterized as an order-of-magnitude agreement. It should also be noted that the experimental values disagree by a factor of two, with no apparent reasons that can be used to explain the differences between the results of determinations in refs¹⁶ and ¹⁸. In light of the uncertainties of the reaction model used in the calculations (discussed in subsection V.2.), the difference between the experimental and the calculated values is not surprising. Considering the fact that a factor of 2 – 4 differences between the experimental values of entropic (preexponential) factors and those derived from

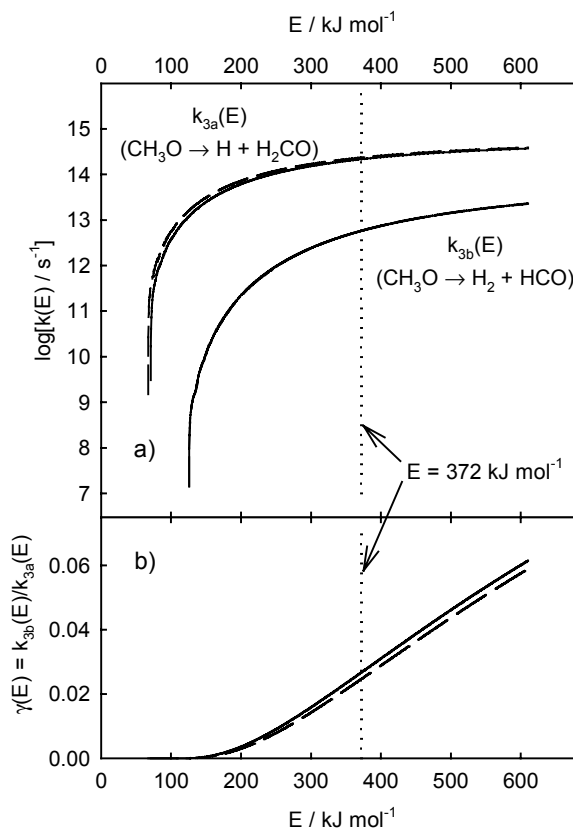


Figure 4. (a) Energy dependences of the microscopic $k(E)$ rates of reaction channels 3a and 3b obtained using the UMP2/6-311G(d,p) potential energy surface with G2 (solid lines) and CBS-Q (dashed lines) energies calculated along the dividing line (PES ridge). The solid and the dashed lines are indistinguishable for the $k_{3b}(E)$ dependence. (b) Energy dependence of the energy-specific branching ratio of channels 3b and 3a, $\gamma(E) = k_{3b}(E)/k_{3a}(E)$. The dotted vertical line on both plots marks the energy (372 kJ mol^{-1}) of the "entrance" channel of the chemically activated $\text{O} + \text{CH}_3 \rightarrow \text{CH}_3\text{O}^* \rightarrow \text{products}$ (1) reaction.

quantum chemistry calculations via transition state theory are not unusual for “ordinary” thermal reactions, the current results of modeling of the reaction of the new “over-the-ridge” type can be described as moderately successful.

References

1. Holbrook, K. A.; Pilling, M. J.; Robertson, S. H. *Unimolecular Reactions*; 2nd ed. Wiley: New York, 1996.
2. Robinson, P. J.; Holbrook, K. A. *Unimolecular Reactions*; Wiley-interscience: New York, 1972.
3. Forst, W. *Theory of Unimolecular Reactions*; Academic Press: New York, 1973.
4. Warnatz, J. in *Combustion Chemistry*; Gardiner, W. C. Jr., Ed. Springer-Verlag: New York, 1984.
5. Warnatz, J.; Mass, U.; Dibble, R. W. *Combustion: Physical and Chemical Fundamentals, Modeling and Simulation, Experiments, Pollutant Formation*; Springer: Berlin, Heidelberg, New York, 1996.
6. Washida, N. *J. Chem. Phys.* **1980**, *73*, 1665.
7. Plumb, I. C.; Ryan, K. R. *Int. J. Chem. Kinet.* **1982**, *14*, 861.
8. Zellner, R.; Hartmann, D.; Karthaus, J.; Rhasa, D.; Weibring, G. *J. Chem. Soc. Faraday Trans. 2* **1988**, *84*, 549.
9. Slagle, I. R.; Sarzynski, D.; Gutman, D. *J. Phys. Chem.* **1987**, *91*, 4375.
10. Oser, H.; Walter, D.; Stothard, N. D.; Grotheer, O.; Grotheer, H. H. *Chem. Phys. Lett.* **1991**, *181*, 521.
11. Lim, K. P.; Michael, J. V. *J. Chem. Phys.* **1993**, *98*, 3919.
12. Bhaskaran, K. A.; Frank, P.; Just, Th. *Proc. Int. Symp. Shock Tubes Waves* **1980**, *12*, 503.
13. Fockenberg, C.; Hall, G. E.; Preses, J. M.; Sears, T. J.; Muckerman, J. T. *J. Phys. Chem. A* **1999**, *103*, 5722.
14. Tsang, W.; Hampson, R. F. *J. Phys. Chem. Ref. Data* **1986**, *15*, 1087.
15. Baulch, D. L.; Cobos, C. J.; Cox, R. A.; Esser, C.; Frank, P.; Just, Th.; Kerr, J. A.; Pilling, M. J.; Troe, J.; Walker, R. W.; Warnatz, J. *J. Phys. Chem. Ref. Data* **1992**, *21*, 411.
16. Seakins, P. W.; Leone, S. R. *J. Phys. Chem.* **1992**, *96*, 4478.
17. Min, Z.; Quandt, R. W.; Wong, T.-H.; Bersohn, R. *J. Chem. Phys.* **1999**, *111*, 7369.
18. Preses, J. M.; Fockenberg, C.; Flynn, G. W. *J. Phys. Chem.* **2000**, *104*, 6758.
19. Slagle, I. R.; Kalinowski, I. J.; Gutman, D.; Harding, L. *Manuscript in Preparation*.
20. Timonen, R. S.; Ratajczak, E.; Gutman, D.; Wagner, A. F. *J. Phys. Chem.* **1987**, *91*, 5325.
21. Wagner, A. F.; Bowman, J. M. *J. Phys. Chem.* **1987**, *91*, 5314.
22. Frisch, M. J.; Trucks, G. W.; Schlegel, H. B.; Scuseria, G. E.; Robb, M. A.; Cheeseman, J. R.; Zakrzewski, V. G.; Montgomery, J. A. Jr.; Stratmann, R. E.; Burant, J. C.; Dapprich, S.; Millam, J. M.; Daniels, A. D.; Kudin, K. N.; Strain, M. C.; Farkas, O.; Tomasi, J.; Barone, V.; Cossi, M.; Cammi, R.; Mennucci, B.; Pomelli, C.; Adamo, C.; Clifford, S.; Ochterski, J.; Petersson, G. A.; Ayala, P. Y.; Cui, Q.; Morokuma, K.; Malick, D. K.; Rabuck, A. D.; Raghavachari, K.; Foresman, J. B.; Cioslowski, J.; Ortiz, J. V.; Baboul, A. G.; Stefanov, B. B.; Liu, G.; Liashenko, A.; Piskorz, P.; Komaromi, I.; Gomperts, R.; Martin, R. L.; Fox, D. J.; Keith, T.; Al-Laham, M. A.; Peng, C. Y.; Nanayakkara, A.; Gonzalez, C.; Challacombe, M.; Gill, P. M. W.; Johnson, B.; Chen, W.; Wong, M. W.; Andres, J. L.; Gonzalez, C.; Head-Gordon, M.; Replogle, E. S.; Pople, J. A. *Gaussian 98, Revision A.7*; Gaussian, Inc.: Pittsburgh, PA, 1998.
23. Fukui, K. *Acc. Chem. Res.* **1981**, *14*, 363.
24. Gonzalez, C.; Schlegel, H. B. *J. Phys. Chem.* **1990**, *94*, 5523.
25. Curtiss, L. A.; Raghavachari, K.; Trucks, G. W.; Pople, J. A. *J. Chem. Phys.* **1991**, *94*, 7221.
26. Ochterski, J. W.; Petersson, G. A.; Montgomery, J. A. *J. Chem. Phys.* **1996**, *104*, 2598.
27. Miller, H. W.; Handy, N. C.; Adams, J. E. *J. Chem. Phys.* **1980**, *72*, 99.
28. Baboul, A. G.; Schlegel, H. B. *J. Chem. Phys.* **1997**, *107*, 9413.
29. Knyazev, V. D. *Manuscript in Preparation*.